

RSC Advances



This is an *Accepted Manuscript*, which has been through the Royal Society of Chemistry peer review process and has been accepted for publication.

Accepted Manuscripts are published online shortly after acceptance, before technical editing, formatting and proof reading. Using this free service, authors can make their results available to the community, in citable form, before we publish the edited article. This *Accepted Manuscript* will be replaced by the edited, formatted and paginated article as soon as this is available.

You can find more information about *Accepted Manuscripts* in the [Information for Authors](#).

Please note that technical editing may introduce minor changes to the text and/or graphics, which may alter content. The journal's standard [Terms & Conditions](#) and the [Ethical guidelines](#) still apply. In no event shall the Royal Society of Chemistry be held responsible for any errors or omissions in this *Accepted Manuscript* or any consequences arising from the use of any information it contains.

A Novel C18 Reversed Phase Organic-Silica Hybrid Cationic Monolithic Capillary Column with Ionic Liquid as Organic Monomer via “One-Pot” Approach for Capillary Electrochromatography

Guozhen Fang, Hailong Qian, Qiliang Deng, Xuqin Ran, Yukun Yang, Cuicui Liu, Shuo Wang*

Key Laboratory of Food Nutrition and Safety, Ministry of Education, Tianjin Key Laboratory of Food Nutrition and Safety, Tianjin University of Science and Technology, Tianjin, 300457, China.

***Corresponding author: Shuo Wang**

Tel: +86 22 6060 1430

Fax: +86 22 6060 1332

Email: s.wang@tust.edu.cn

Abbreviations: IL, ionic liquid; $\text{VC}_{18}\text{HIm}^+\text{Br}^-$, 1-vinyl-3-dodecylimidazolium bromide; VTES, triethoxyvinylsilane; TEOS, tetraethyl orthosilicate; EGDMA, ethylene dimethacrylate; i-PrOH, isopropanol; n-BuOH, n-Butanol; MeOH, methanol; EA, element analysis; DDW, doubly deionized water; cLC, capillary liquid chromatography

Keywords: Capillary electrochromatography, Hybrid cationic monolithic column, Ionic liquid, One-pot, Reversed phase

ABSTRACT

A novel C18 reversed phase (RP) organic-silica hybrid cationic monolithic capillary column with ionic liquid (IL) as organic monomer has been fabricated by “one-pot” approach for capillary electrochromatography (CEC). Through copolymerization, the IL 1-vinyl-3-octadecylimidazolium bromide ($\text{VC}_{18}\text{HIm}^+\text{Br}^-$) was successfully anchored into the monolithic matrix which was formed through polycondensation of tetraethyl orthosilicate (TEOS) and triethoxyvinylsilane (VTES). Several experimental variables, which were essential to the preparation of the columns, such as TEOS/VTES ratio, content of H_2O and supermolecule template, amount of IL and polycondensation temperature were studied in detail, and three control columns were prepared to compare with this prepared novel hybrid monolithic column. Separation of various neutral, charged and basic analytes as well as protein sample on the $\text{VC}_{18}\text{HIm}^+\text{Br}^-$ hybrid monolithic column and control columns was achieved by CEC. It was found that the prepared hybrid monolithic column possessed its own superiority in separation. Besides, the retention mechanism of neutral analytes on this column was typical reversed phase chromatographic retention mechanism, and the separation of charged compounds depended on the combination of electrophoretic mobility, ionic exchange interaction and hydrophobic interaction. Moreover, the prepared hybrid monolithic column also settled the problem of peak tailing for separating the basic analytes, and the separation of egg white demonstrated its potential in proteome analysis.

1. Introduction

With the rapid development of analytical chemistry, more complex mixtures are needed to be separated. The requirement of novel separation systems with excellent separation ability is becoming more urgent. Capillary electrochromatography (CEC) demonstrates its distinct merits in satisfying the requirement as it combines various merits of both high performance liquid chromatography (HPLC) and capillary electrophoresis (CE).^{1,2} As the “heart” of the CEC system, the capillary columns provide the driving force as well as the separation medium.^{3,4} Consequently, the preparation of CEC columns makes phenomenal progress in the past few decades. The monolithic columns, the most promising CEC columns, have been attracting more attention due to their unique properties including easy preparation, good permeability and fast mass transfer.⁵⁻⁷ According to the types of monolithic matrix, the monolithic columns are mainly categorized into three major types: silica-based monolithic columns, organic polymer-based monolithic columns and organic-silica hybrid monolithic columns.^{8,9} Considered to be the new burgeoning monolithic columns, the organic-silica hybrid monolithic columns combine the advantages of two former classes columns,^{10,11} and have been becoming the primary monolithic columns recently.

Since Malik et al. fabricated a hybrid monolithic column via sol-gel reaction for the first time,¹² many approaches have already been developed in the preparation of organic-silica hybrid monolithic columns. The advanced “one-pot” approach is one of the most widely utilized methods currently which contains two thermal treatments,¹³ the sol-gel process occurs at low temperature to achieve uniform porous monolithic matrix, and the subsequent copolymerization occurs at a relatively high temperature

68 to make the monomer incorporate into the monolithic matrix. This new method
69 overcomes one drawback of traditional sol-gel reaction that the functional monomer
70 must be silane reagent,^{14,15} making it possible to use ionic liquids (ILs) as organic
71 monomers.

72 ILs are a new type molten salts with many unique physical and chemical
73 characteristics,^{16,17} including low melting point, non-volatility, high ionic
74 conductivity, available design and high thermal stability, which make them easy to be
75 utilized in chemical analysis field. So far, ILs have been applied as mobile phase
76 additives to improve the shape of chromatographic peak and the separation
77 efficiency.^{18,19} In the preparation of monolith, ILs also have been used as stationary
78 phase coatings to reverse the direction of electroosmotic flow (EOF) for better
79 separation of analytes.^{20,21} Besides, Li et al.²² have reported that the ILs can assistant
80 to form simultaneously the through pores and mesopores during the sol-gel reaction.
81 Yan et al.²³ used ILs as pore template and to reduce gel shrinkage in the preparation
82 of molecularly imprinted silica-based hybrid monoliths for chiral separation.
83 Recently, ILs are used as the functional monomers for preparation of the organic
84 polymer-based monolithic columns.²⁴ Liu et al.²⁵ prepared a PIL modified
85 (PImC8-silica) hybrid monolithic column with IL as functional monomer which was
86 succeed in separated aromatic hydrocarbons, alkylbenzenes and phenols.

87 Although the applications of ILs in monolith were reported, ILs were mostly used
88 as assisted component to reverse the EOF or tailor mesopores in order to improve the
89 separation efficiency. Few previous works were reported by using ILs as functional
90 monomer, and the preparation processes were tedious which always contained two
91 steps. Firstly, a silica monolithic column was prepared, and then ILs were pumped
92 into the prepared column for further modification. Here, an organic-silica hybrid

monolithic capillary column with IL as functional monomer was fabricated via “one-pot” approach. This work not only simplified the preparation of ILs monolith, but also used ILs to provide both function groups to enhance the selective of neutral compounds and charged groups to reverse the EOF in CEC mode.

As we know, octadecylsilane (C18) stationary phase is one of the most widely used non-polar phase owe to its great resolving ability for a wide range of analytes.²⁶ Hence, 1-vinyl-3-octadecylimidazolium bromide ($\text{VC}_{18}\text{HIm}^+\text{Br}^-$) was chosen in this work and the $\text{VC}_{18}\text{HIm}^+\text{Br}^-$ hybrid monolithic column was successfully prepared via “one-pot” approach. Three control columns were prepared to investigate the superiority of the prepared $\text{VC}_{18}\text{HIm}^+\text{Br}^-$ hybrid column. Moreover, a series of characterizations and chromatographic experiments indicated the prepared $\text{VC}_{18}\text{HIm}^+\text{Br}^-$ hybrid monolithic capillary columns possess a promising prospect for broad applications.

2. Experimental

2.1. Chemicals and materials

1-vinyl-3-octadecylimidazolium bromide ($\text{VC}_{18}\text{HIm}^+\text{Br}^-$) was purchased from Lanzhou Institute of Chemical Physics (Lanzhou, China). Tetraethyl orthosilicate (TEOS), Ethylene dimethacrylate (EGDMA) and Triethoxyvinylsilane (VTES) were obtained from Sigma (St. Louis, MO, USA). Azobisisobutyronitrile (AIBN) was purchased from Tianjin Chemical Reagent Factory (Tianjin, China) and recrystallized in ethanol before utilization. Cetyltrimethylammonium bromide (CTAB) was purchased from Aobox Biotechnology Co., Ltd. (Tianjin, China). Isopropanol (i-PrOH) and n-Butanol (n-BuOH) were obtained from Sinopharm Chemical Reagent

Co., Ltd. (Shanghai, China). Doubly deionized water (DDW, $18 \text{ M}\Omega \text{ cm}^{-1}$) used throughout the experiment was manufactured by a Milli-Q system (Millipore Corporation, USA). HPLC-grade methanol (MeOH) and acetonitrile (ACN) used as mobile phases were purchased Merck KGaA (Darmstadt, Germany). Fused-silica capillary (100 μm i.d., 375 μm o.d.) was purchased from Refine Chromatography Ltd. (Hebei, China).

2.2. Apparatus

The Fourier transform infrared (FT-IR) spectra with KBr pellets (4000–400 cm^{-1}) were achieved by a Vector 22 spectrometer (Bruker, Germany). Scanning electron microscopy (SEM) images of the monoliths were obtained on a SU1510 SEM (Hitachi, Japan). Elementary analysis (EA) was performance on Vario MACRO cube (ELEMENTAR, German). The capillary liquid chromatography (cLC) experiments were performed on an Agilent 1100 LC system (Agilent, USA). CEC experiments were performed on P/ACE MDQ CE system (Beckman-Coulter, USA) equipped with a UV detector which was controlled by Beckman ChemStation software.

2.3. Procedures for cLC and CEC

All data obtained were based on three runs. The mobile phase must be filtered by a 0.22 μm membrane and degassed by ultrasonic before used on cLC.

The $\text{VC}_{18}\text{HIm}^+\text{Br}^-$ hybrid monolithic capillary columns must be conditioned for at least 30 min on cLC with buffers prior to the CEC experiment. Every time before separation, the columns were equilibrated until an unfluctuating current was achieved. All the solutions loading into the CE system must be filtered with 0.22 μm membrane and degassed by ultrasonic. The total separation was carried out at room temperature.

139 2.4. Preparation of the $\text{VC}_{18}\text{HIm}^+\text{Br}^-$ hybrid monolithic capillary column

140 According to the “one-pot” process reported previously,¹³ the fused-silica capillary
141 must be pretreated to make the capillary inner wall expose more Si-OH for the
142 subsequent attachment of monolith. Firstly, the fused-silica capillary was handled
143 with 1.0 M NaOH for 12 h, DDW for 30 min, 1.0 M HCl for 12 h, DDW for another
144 30 min, MeOH for 30 min, respectively, and then dried in a nitrogen stream at room
145 temperature for further use.

146 The prepolymerization mixture containing i-PrOH (500 μL), n-BuOH (100 μL),
147 water (110 μL), TEOS (300 μL), VTES (200 μL), CTAB (5 mg), AIBN (5 mg), 1.0 M
148 ammonia water (50 μL) and $\text{VC}_{18}\text{HIm}^+\text{Br}^-$ (150 mg) was stirred and sonicated for 10
149 min, respectively, to obtain homogenous solution at room temperature. The solution
150 was artificially poured into 36 cm long pretreated capillary to a suitable length with
151 syringe. After both ends of the capillary were sealed with rubbers, the capillary was
152 incubated at 40 °C water for 12 h for polycondensation of TEOS and VTES, and then
153 the capillary was continuously incubated at 60 °C water for another 12 h for
154 incorporation of $\text{VC}_{18}\text{HIm}^+\text{Br}^-$. At last, the prepared monolithic capillary columns
155 were connected to the cLC and rinsed with i-PrOH and n-BuOH to remove CTAB and
156 other residuals, and a detection window was made at the end of capillary columns.

157 Several control columns were prepared to compare with the prepared $\text{VC}_{18}\text{HIm}^+\text{Br}^-$
158 hybrid column, and the preparation of control columns was showed in Supporting
159 Information.

160 3. Results and discussion

161 **3.1. Optimization of synthetic conditions for the $\text{VC}_{18}\text{HIm}^+\text{Br}^-$ hybrid monolithic**
162 **capillary column**

163 As shown in Table 1, several experimental variables such as TEOS/VTES ratio,
164 content of H_2O , amount of supermolecule template (CTAB) and polycondensation
165 temperature were investigated in detail.

166 In the processes of hydrolysis and polycondensation of alkoxysilanes, the effect of
167 TEOS/VTES ratio on the formation of monolith was investigated by varying its
168 volume ratios from 300/150 to 300/250. As seen from Table 1, the low content of
169 VTES (column A2, TEOS/VTES = 300/150) would decrease the content of $\text{C}=\text{C}$
170 double bonds which was essential to the subsequent bond of $\text{VC}_{18}\text{HIm}^+\text{Br}^-$, while the
171 high content of VTES (column A3, TEOS/VTES = 300/250) would result in layering
172 phenomenon and poor permeability of monolith, and the mobile phase was hard to be
173 pumped through the column A3. Only when the volume ratio was at 300/200 (column
174 A1), can a uniform and non-transparent monolith with excellent permeability be
175 produced.

176 Because of the vital effect on the hydrolysis of alkoxysilanes, the content of water
177 was also optimized and the results were reflected by column B1 (110 μL), column B2
178 (50 μL) and column B3 (140 μL). As shown in Table 1, the matrix of column B2
179 detached seriously due to the incomplete hydrolysis of alkoxysilanes without enough
180 water. However, with content of water increasing, the reaction solution would become
181 more and more incompatible for the high hydrophobicity of IL. So the reactant
182 solution of column B3 seriously stratified which led to the failing formation of
183 monolith. In contrast, the matrix of column B1 was acceptable and the 110 μL water
184 could ensure not only the complete hydrolysis of alkoxysilanes but also the stability
185 of the reactant system.

186 The CTAB was used as both surfactant and supramolecular template in the process
187 of sol-gel reaction. According to Yan et al's work,²⁷ it proved that the formation of
188 organic-silica hybrid mesostructure was the result of the delicate balance of two
189 competitive processes-organizations of the template and polymerization. A series of
190 columns C1 (5 mg CTAB), column C2 (3 mg CTAB) and column C3 (9 mg CTAB)
191 in Table 1 were produced to study the effect of CTAB on the formation of monolith.
192 The results showed that the low amount of CTAB resulted in the poor permeability of
193 the column, while the high one substantially deteriorated the efficiency of the column.
194 Correspondingly, the matrix of column C2 was inhomogeneous and that of column
195 C3 was slacked. Only the column C1 exhibited a desirable monolith. Hence, 5 mg
196 CTAB was proved to be the best condition in this reactant system.

197 As the temperature had significant effect on the formation of monolithic matrix,
198 columns D1, column D2, column D3 were fabricated at 40 °C, 35 °C, 45 °C,
199 respectively, to research the tendency of the temperature effect. It was found the
200 monolithic matrix of column D2 (35 °C) was nonrigid and seriously detached from
201 the capillary inner wall, which attributed to the incomplete polycondensation of the
202 alkoxysilanes. With the increase of temperature, the structure of monolith gradually
203 became solid. When the temperature was 40 °C, a uniform monolithic matrix (column
204 D1) tightly bonded onto the capillary inner wall was achieved. Continuously
205 increasing the temperature to 45 °C, the monolith (column D3) became too solid to
206 allow the mobile phase flow through. Accordingly, the 40 °C was employed in this
207 work.

208 In order to ensure the amount of the $\text{VC}_{18}\text{HIm}^+\text{Br}^-$, the μ_{EOF} and k' were chosen as
209 evaluating standard. The μ_{EOF} was calculated by the equation $\mu_{\text{EOF}} = L_e L_t / (V t_0)$, where
210 L_t is the total length of column, L_e is the effective length of column, V is the applied

211 voltage, t_0 is the elution time of unretained compound (thiourea), and the k' was
212 calculated by the equation $k' = (t_r - t_0)/t_0$, where t_r is the retention time of analyte, t_0 is
213 the elution time of unretained compound (thiourea). During the experiment, it was
214 found the maximum dissolution of $\text{VC}_{18}\text{HIm}^+\text{Br}^-$ in the optimal solution was 200 mg.
215 Hence, a number of columns with 100 mg, 125 mg, 150 mg, 200 mg $\text{VC}_{18}\text{HIm}^+\text{Br}^-$
216 were prepared to confirm the best amount of $\text{VC}_{18}\text{HIm}^+\text{Br}^-$. According to the results,
217 with the amount of $\text{VC}_{18}\text{HIm}^+\text{Br}^-$ increasing, the μ_{EOF} decreased obviously from 2.53
218 $\times 10^{-4} \text{ cm}^2 \text{ v}^{-1} \text{ s}^{-1}$ to $1.33 \times 10^{-4} \text{ cm}^2 \text{ v}^{-1} \text{ s}^{-1}$, and the columns prepared with 200 mg
219 $\text{VC}_{18}\text{HIm}^+\text{Br}^-$ were even blocked, owing to the fact that overfull IL had an adverse
220 effect on the permeability of the column. On the contrary, the k' for benzene increased
221 from 0.671 to 0.989. In consideration of the common effect of $\text{VC}_{18}\text{HIm}^+\text{Br}^-$ on μ_{EOF}
222 and k' , 150 mg $\text{VC}_{18}\text{HIm}^+\text{Br}^-$ would be the best choice in this work.

223 Due to high hydrophobic property of the functional monomer $\text{VC}_{18}\text{HIm}^+\text{Br}^-$,
224 i-PrOH and n-BuOH were chosen as the solvent, and a highly stable transparent
225 reactant system was achieved when the volume ratio of i-PrOH/n-BuOH was 500/100
226 (v/v). The concentration of ammonia water played an important role in the sol-gel
227 reaction. It was found the matrix could be formed after 12 h reaction when the
228 concentration of ammonia water was 0.5 M, but the prepared matrix was non-rigid.
229 With the concentration of ammonia water increasing, the matrix became more and
230 more rigid, and the rate of condensation increased as well. When the concentration
231 was 2 M, the reaction mixture quickly became solid, and there was no enough time to
232 inject the mixture into the capillary. It was proved that the optimal concentration was
233 1 M in this work.

234 **3.2. Characterization of the optimized the $\text{VC}_{18}\text{HIm}^+\text{Br}^-$ hybrid monolithic**
235 **capillary column**

236 The FT-IR was used to prove the anchor of $\text{VC}_{18}\text{HIm}^+\text{Br}^-$ to the monolithic matrix.
237 As showed in Fig. 1, some characteristic peaks of $\text{VC}_{18}\text{HIm}^+\text{Br}^-$ were observed
238 clearly at $2927, 2850\text{ cm}^{-1}$ ($-(\text{CH}_2)_n-$), 1650 cm^{-1} ($\text{C}=\text{C}$) and 1550 cm^{-1} ($\text{C}=\text{N}$) in Fig.
239 1(I). Comparing with the other two FT-IR photographs, the IL characteristic peaks of
240 $-(\text{CH}_2)_n-$ at $2929, 2851\text{ cm}^{-1}$ and $\text{C}=\text{N}$ at 1552 cm^{-1} shown in Fig. 1(III) were not
241 appeared in Fig. 1(II) indicating that the $\text{VC}_{18}\text{HIm}^+\text{Br}^-$ groups were successfully
242 incorporated into the silica-based monolith.

243 The EA results of the monoliths with different amount of $\text{VC}_{18}\text{HIm}^+\text{Br}^-$ were
244 showed in Table. 2. According to the results, the monolith prepared without
245 $\text{VC}_{18}\text{HIm}^+\text{Br}^-$ only contained 0.08% nitrogen which may result from the residuals of
246 CTAB and AIBN. Correspondingly, the nitrogen proportion of $\text{VC}_{18}\text{HIm}^+\text{Br}^-$
247 monolith was increased apparently (1.18%), and with the amount of $\text{VC}_{18}\text{HIm}^+\text{Br}^-$
248 increasing, the N% also increased from 1.18% to 1.66%. As a consequence, the results
249 proved the successful copolymerization of $\text{VC}_{18}\text{HIm}^+\text{Br}^-$ and the monolith.

250 The SEM photographs of $\text{VC}_{18}\text{HIm}^+\text{Br}^-$ hybrid monolithic capillary column were
251 shown in Fig. 2. It can be seen that a uniform porous monolithic matrix tightly
252 anchored to the inner capillary wall through the 600 times magnification condition.
253 Besides, with 6000 times magnification, the matrix was constructed by plenty of small
254 particles, which could increase the rate of mass transfer due to the increasing of
255 contact area with samples during the separation.

256 With thiourea as the EOF maker, the relationship of mobile phase pH and the EOF
257 of was investigated. According to the Fig. 3, the prepared hybrid column could
258 maintain strong anodic EOF in a wide range of pH (3.0–11.0), which was due to the
259 existence of strong cationic imidazole groups. The permeability of the $\text{VC}_{18}\text{HIm}^+\text{Br}^-$
260 hybrid monolithic capillary columns was investigated by the Darcy's Law²⁸ $B_0 =$

261 $F\eta L/(\pi r^2 \Delta P)$, where F is the flow rate of the mobile phase, η is the viscosity of the
262 mobile phase, L is the effective length of column, r is the inner radius of the column,
263 and ΔP is the pressure drop of the column. Using ACN ($\eta = 0.38$ cP) as the mobile
264 phase, the permeability of the hybrid monolithic column was calculated to be $5.28 \times$
265 10^{-14} m^2 . The mechanical stability of the $\text{VC}_{18}\text{HIm}^+\text{Br}^-$ hybrid monolithic capillary
266 column was examined by connecting columns to cLC using ACN as the mobile phase.
267 As the results showed in Fig. 4A, with the flow rate ranged from $0.5 \mu\text{L min}^{-1}$ to 10
268 $\mu\text{L min}^{-1}$, the backpressure increased linearly from 11 bar to 185 bar with relation
269 factor of 0.9999. The column efficiency of the $\text{VC}_{18}\text{HIm}^+\text{Br}^-$ hybrid monolithic
270 capillary columns was evaluated by Van Deemter curve, which was shown Fig. 4B.
271 Using toluene as test sample, A minimum plate height of $5.58 \pm 0.22 \mu\text{m}$
272 corresponding to 179211 ± 7060 theoretical plates per meter was obtained.

273 In order to prove the advantages of this work, a series of control columns (the
274 preparation showed in Supporting Information) were prepared to compare with the
275 $\text{VC}_{18}\text{HIm}^+\text{Br}^-$ hybrid monolithic capillary column. According to the Supplementary
276 Fig. 1 (Supporting Information), the prepared hybrid monolithic capillary column
277 could form a stable EOF, and the direction of EOF in the column was reversed. The
278 control column 2 and 3 also formed EOF under reversed voltage, while there was no
279 EOF in control column 1, which may result from no charged group on the matrix. The
280 results indicated the IL was the essential factor in the formation of EOF. Under the
281 same calculating condition with the $\text{VC}_{18}\text{HIm}^+\text{Br}^-$ hybrid monolithic column, the
282 permeability of control column 1, 2 and 3 were calculated to be $8.06 \times 10^{-14} \text{ m}^2$, 4.32
283 $\times 10^{-14} \text{ m}^2$ and $7.59 \times 10^{-14} \text{ m}^2$, respectively, and the relation factor for backpressure
284 and flow rate of control column 1, 2 and 3 were determined as 0.9996, 0.9986, 0.9992,
285 respectively. Due to absence of EOF, the column efficiency of control column 1

cannot be achieved, while that of control column 2 and 3 were calculated to be 136798 ± 5677 theoretical plates per meter and 110879 ± 4139 theoretical plates per meter. Accordingly, the IL was the essential factor on the formation of EOF and the VC₁₈HIm⁺Br⁻ hybrid monolithic column prepared by “one-pot” approach possessed its own superiority in the permeability, mechanical stability and column efficiency.

The repeatability and reproducibility of the VC₁₈HIm⁺Br⁻ hybrid monolithic capillary columns were investigated through the relative standard deviation (RSD) of the retention time for benzene. the RSD of the run-to-run ($n = 7$) and day-to-day ($n = 4$) repeatability were 0.48% and 1.16%, respectively, and the RSD of the column-to-column ($n = 3$) and batch-to-batch ($n = 3$) were 3.02% and 3.94% respectively indicating that the hybrid monolithic capillary columns via “one-pot” approach owned not only stable separation repeatability but also satisfied reproducibility.

3.3. Chromatographic evaluation of the optimized VC₁₈HIm⁺Br⁻ hybrid monolithic capillary column

A mixture of alkylbenzenes was used to investigate the separation properties of the VC₁₈HIm⁺Br⁻ hybrid monolithic capillary columns by CEC. As shown in Fig. 5A, the alkylbenzenes were well separated and the analytes were eluted in the order of thiourea < benzene < toluene < ethylbenzene < propylbenzene < butylbenzene according to their polarity from high to low, and with the increase of separation voltage, the separation time reduced rapidly. In addition, the effect of different ACN content on the retention factors of alkylbenzenes was investigated and the results were exhibited in Fig. 5B. It was found that the retention factors of alkylbenzenes decreased with the content of ACN increasing in the buffer. Consequently the

310 separation of alkylbenzenes on the $\text{VC}_{18}\text{HIm}^+\text{Br}^-$ hybrid monolithic capillary columns
311 mainly based on typical reversed phase chromatographic retention mechanism

312 The amino acids mixture (aspartic acid $\text{pI} = 2.77$, glutamic acid $\text{pI} = 3.22$,
313 L-phenylalanine $\text{pI} = 5.48$, glutamine $\text{pI} = 5.65$ and L-proline $\text{pI} = 6.30$) was chosen
314 to investigate the separation of charged analytes on the $\text{VC}_{18}\text{HIm}^+\text{Br}^-$ hybrid
315 monolithic capillary columns. As shown in Fig. 6A, the amino acids were baseline
316 separated with the elution order aspartic acid < glutamic acid < glutamine < L-proline
317 < L-phenylalanine. In order to acquaint the retention mechanism of the charged
318 mixture, the same amino acids mixture was separated in different pH, salt
319 concentration and content of ACN. In the Supplementary Fig. 2a, due to the only
320 negatively charged amino acids was the aspartic acid at pH 3.0, its electrophoretic
321 migration was identical to EOF resulting in the headmost elution of the aspartic acid.
322 When pH of the mobile phase was 5.0, the glutamic acid also became negatively
323 charged. Thus, it brought the reduction retention time of glutamic acid and the
324 improvement of separation, which was showed in Supplementary Fig. 2b. At last,
325 with the continuous increase of pH to 7.0, all the amino acids became negatively
326 charged. Correspondingly, the retention times of all the amino acids shortened
327 obviously which was consistent with Supplementary Fig. 2c. Through the change of
328 salt concentration, the retention mechanism of ionic exchange was studied. Through
329 the Supplementary Fig. 3a, it can be seen the amino acids were separated, when the
330 salt concentration was 40 mM. As the increase of salt concentration to 50 mM, the
331 retention time of all the amino acids decreased and the peak of aspartic acid
332 overlapped with glutamic acid. When the salt concentration was 60 mM, the retention
333 time of all the amino acids continued to decrease, and the separation also deteriorated
334 obviously. Since the ionic exchange interaction could be suppressed by higher salt

concentration to some extent, the results could demonstrate that ionic exchange existed in the separation process. What's more, the results of different ACN content effect on the separation were showed in Supplementary Fig. 4. The retention time of all the amino acids decreased with the increase of the ACN content, which indicated the hydrophobic interaction was also one of the mechanisms during the separation. In summary, the retention mechanism of the prepared $\text{VC}_{18}\text{HIm}^+\text{Br}^-$ monolithic capillary columns for charged compounds is the combination of electrophoretic mobility, ionic exchange interaction, and hydrophobic interaction.

Since the separation of basic compounds is always suffered from peak tailing due to the nonspecific absorption between basic analytes and silica monolithic matrix in previous reports.²⁹ The $\text{VC}_{18}\text{HIm}^+\text{Br}^-$ monolithic capillary columns were also applied to separate the basic compounds (methimazole, aniline, gramine, 1,2-diphenylhydrazine). As shown in Fig. 6B, the basic compounds were baseline separated with good peak shape. The conventional peak tailing problem didn't appear as a result of the repression of positively charged imidazole groups on the nonspecific absorption mentioned above.

The control columns were also applied to separate the same neutral, charged and basic analytes under the same condition with the prepared hybrid monolithic column, and the results and interpretations were showed in Supporting Information (the data of control column 1 cannot be obtained for no EOF). As see from the Supplementary Fig. 5, the separation of alkylbenzenes on the control columns was undesirable. Although the retention of benzene, toluene, ethylbenzene and propylbenzene on control column 2 was acceptable, the peak broadening of butylbenzene was serious, and the column efficiency of control column 3 for the alkylbenzenes was not high. According to Supplementary Fig. 6, the glutamine and L-proline was not separated by

the control column 2, while all the amino acids was separated on the control column 3, but the peak of the aspartic acid and glutamic acid was too close and the shape of all the peaks was asymmetrical. As to the basic compounds, the peak tailing problem was not appear which was showed in Supplementary Fig. 7. However, the retention for the basic compounds was weak on the control columns compared with the hybrid monolithic column prepared with “one-pot” in this work. Hence, it can be achieved that the comprehensive separation ability of $\text{VC}_{18}\text{HIm}^+\text{Br}^-$ hybrid monolithic capillary column was outstanding.

To evaluate the potential proteome analysis of the prepared column, the $\text{VC}_{18}\text{HIm}^+\text{Br}^-$ hybrid monolithic capillary columns were further applied to separate egg white. As shown in Fig. 7, it can be found 7 major peaks were detected with no organic solvent and additives in mobile phase, which was friendly for protein, demonstrating potential separation of the prepared columns on the proteins compared with the previous report.³⁰

4. Conclusion

The $\text{VC}_{18}\text{HIm}^+\text{Br}^-$ hybrid monolithic capillary columns with desirable morphology were obtained in this work. Moreover, the prepared columns were applied in the analysis of various neutral, charged and basic analytes as well as protein sample, and further compared with a series of control columns. All these results indicated that the fabricated columns would be of great potential in separation area.

381 **Acknowledgments**

382 This work was supported by the Ministry of Science and Technology of China
383 (Project No. 2012AA101609-2) and the National Natural Science Foundation of
384 China (Project No. 21375094 and 21075089) and General Administration of Quality
385 Supervision, Inspection and Quarantine of the People’s Republic of China (Project
386 No. 201210053) and the Program for Changjiang Scholars and Innovative Research
387 Team in University (Project no. IRT1166).

388

389 **5. Reference**

- 390 1. I. Krull, A. Sebag and R. Stevenson, *J. Chromatogr., A*, 2000, 887, 137-163.
- 391 2. J. Knox and I. Grant, *Chromatographia*, 1987, 24, 135-143.
- 392 3. M. Pursch and L. C. Sander, *J. Chromatogr., A*, 2000, 887, 313-326.
- 393 4. Q. Tang and M. L. Lee, *Trac-trend Anal. Chem.*, 2000, 19, 648-663.
- 394 5. F. Svec, E. C. Peters, D. Sýkora and J. M. Fréchet, *J. Chromatogr., A*, 2000, 887,
- 395 3-29.
- 396 6. H. Zou, X. Huang, M. Ye and Q. Luo, *J. Chromatogr., A*, 2002, 954, 5-32.
- 397 7. M. M. Wang, H. F. Wang, D. Q. Jiang, S. W. Wang and X. P. Yan,
- 398 *Electrophoresis*, 2010, 31, 1666-1673.
- 399 8. I. Gusev, X. Huang and C. Horváth, *J. Chromatogr., A*, 1999, 855, 273-290.
- 400 9. G. Guiochon, *J. Chromatogr., A*, 2007, 1168, 101-168.
- 401 10. M. Wu, R. a. Wu, Z. Zhang and H. Zou, *Electrophoresis*, 2011, 32, 105-115.
- 402 11. L. Bai, H. Liu, Y. Liu, X. Zhang, G. Yang and Z. Ma, *J. Chromatogr., A*, 2011,
- 403 1218, 100-106.
- 404 12. J. D. Hayes and A. Malik, *Anal. Chem.*, 2000, 72, 4090-4099.
- 405 13. H. Lin, J. Ou, Z. Zhang, J. Dong, M. Wu and H. Zou, *Anal. Chem.*, 2012, 84,
- 406 2721-2728.
- 407 14. M. Wu, R. a. Wu, F. Wang, L. Ren, J. Dong, Z. Liu and H. Zou, *Anal. Chem.*,
- 408 2009, 81, 3529-3536.

- 409 15. Z. Zhang, M. Wu, R. a. Wu, J. Dong, J. Ou and H. Zou, *Anal. Chem.*, 2011, 83,
410 3616-3622.
- 411 16. H. Ohno, M. Yoshizawa and W. Ogihara, *Electrochimi. Acta*, 2004, 50, 255-261.
- 412 17. T. Welton, *Chem. Rev.*, 1999, 99, 2071-2084.
- 413 18. M. Ruiz-Angel, S. Carda-Broch and A. Berthod, *J. Chromatogr., A*, 2006, 1119,
414 202-208.
- 415 19. W. Zhang, L. He, Y. Gu, X. Liu and S. Jiang, *Anal. Lett.*, 2003, 36, 827-838.
- 416 20. W. Qin, H. Wei and S. F. Y. Li, *J. Chromatogr., A*, 2003, 985, 447-454.
- 417 21. M. Borissova, M. Vaher, M. Koel and M. Kaljurand, *J. Chromatogr., A*, 2007,
418 1160, 320-325.
- 419 22. J. Chen, P. Zhang and L. Jia, *J. Chromatogr., A*, 2011, 1218, 3699-3703.
- 420 23. H. F. Wang, Y. Z. Zhu, X. P. Yan, R. Y. Gao and J. Y. Zheng, *Adv. Mater.*, 2006,
421 18, 3266-3270.
- 422 24. Y. Wang, Q. L. Deng, G. Z. Fang, M. F. Pan, Y. Yu and S. Wang, *Anal. Chim.*
423 *Acta*, 2012, 712, 1-8.
- 424 25. H. Han, Q. Wang, X. Liu and S. Jiang, *J. Chromatogr., A*, 2012, 1246, 9-14.
- 425 26. Z. Zhang, H. Lin, J. Ou, H. Qin, R. a. Wu, J. Dong and H. Zou, *J. Chromatogr., A*,
426 2012, 1228, 263-269.
- 427 27. L. Yan, Q. Zhang, J. Zhang, L. Zhang, T. Li, Y. Feng, L. Zhang, W. Zhang and Y.
428 Zhang, *J. Chromatogr., A*, 2004, 1046, 255-261.
- 429 28. R. D. Stanelle, L. C. Sander and R. K. Marcus, *J. Chromatogr., A*, 2005, 1100,
430 68-75.

431 29. X. Wang, K. Ding, C. Yang, X. Lin, H. Lü, X. Wu and Z. Xie, *Electrophoresis*,

432 2010, 31, 2997-3005.

433 30. Q. Qu, C. Gu, Z. Gu, Y. Shen, C. Wang and X. Hu, *J. Chromatogr., A*, 2013.

434

435 **Fig. 1.** FT-IR spectra of (I) IL ($\text{VC}_{18}\text{HIm}^+\text{Br}^-$), (II) the silica-based monolith without
436 IL and (III) the $\text{VC}_{18}\text{HIm}^+\text{Br}^-$ hybrid monolith.

437 **Fig. 2.** SEM images of $\text{VC}_{18}\text{HIm}^+\text{Br}^-$ hybrid monolithic capillary column with
438 optimal condition. Magnification: (A) $\times 6000$ and (B) $\times 600$.

439 **Fig. 3.** Effect of pH on EOF of the $\text{VC}_{18}\text{HIm}^+\text{Br}^-$ hybrid monolithic capillary column.
440 Experimental conditions: column dimension, $20\text{ cm} \times 100\text{ }\mu\text{m}$ i.d.; injection, -0.5 psi
441 for 5 s ; mobile phase, 30 mM phosphate buffer ($\text{H}_3\text{PO}_4 - \text{Na}_2\text{HPO}_4$ for $\text{pH } 3.0-5.0$,
442 $\text{Na}_2\text{HPO}_4 - \text{NaH}_2\text{PO}_4$ for $\text{pH } 5.0-9.0$, $\text{Na}_2\text{HPO}_4 - \text{NaOH}$ for $9.0-11.0$) containing 30%
443 ACN; void time marker of EOF, thiourea; separation voltage, -10 kV ; detection
444 wavelength, 214 nm .

445 **Fig. 4.** (A) The mechanical stability of the $\text{VC}_{18}\text{HIm}^+\text{Br}^-$ hybrid monolithic capillary
446 column and (B) relationship between linear velocity and the plate height of the
447 prepared column. Experimental conditions: (A) column dimension, $20\text{ cm} \times 100\text{ }\mu\text{m}$
448 i.d.; flow rate $0.5\text{ }\mu\text{L min}^{-1}$ – $10\text{ }\mu\text{L min}^{-1}$ for ACN; (B) column dimension, $20\text{ cm} \times$
449 $100\text{ }\mu\text{m}$ i.d.; injection, -0.5 psi for 5 s ; mobile phase, ACN/ 30 mM acetic acid buffer
450 at $\text{pH } 3.0 = 30/70\text{ (v/v)}$; separation voltage, from -4 kV to -10 kV ; detection
451 wavelength, 214 nm .

452 **Fig. 5.** (A) Separation of alkylbenzenes on the $\text{VC}_{18}\text{HIm}^+\text{Br}^-$ hybrid monolithic
453 capillary column at different separation voltage by CEC and (B) effect of ACN
454 content in the mobile phase on the retention factors of alkylbenzenes. Solutes: (A), (0)
455 thiourea, (1) benzene, (2) toluene, (3) ethylbenzene, (4) propylbenzene, (5)
456 butylbenzene. Experimental conditions: column dimension, $20\text{ cm} \times 100\text{ }\mu\text{m}$ i.d.;
457 mobile phase: (A) ACN/ 30 mM acetic acid buffer at $\text{pH } 3.0 = 40/60\text{ (v/v)}$, (B)
458 different content ACN in 30 mM acetic acid buffer at $\text{pH } 3.0$; injection, -0.5 psi for 5

459 s; separation voltage: (A) different voltage, (B) -10 kV; detection wavelength, 214
460 nm.

461 **Fig. 6.** (A) Separation of amino acids and (B) basic compounds on the $\text{VC}_{18}\text{HIm}^+\text{Br}^-$
462 hybrid monolithic capillary column by CEC. Solutes: (A) (1) aspartic acid, (2)
463 glutamic acid, (3) glutamine, (4) L-proline, (5) L-phenylalanine; (B) (1) methimazole,
464 (2) aniline, (3) gramine, (4) 1,2-diphenyl hydrazine. Experimental conditions: column
465 dimension, $20\text{ cm} \times 100\text{ }\mu\text{m}$ i.d.; injection: (A) -1.0 psi for 15 s, (B) -0.5 psi for 5 s;
466 separation voltage: (A) -5 kV, (B) -10 kV; detection wavelength: (A) 190 nm, (B)
467 214 nm; mobile phase: (A) 40 mM $\text{H}_3\text{PO}_4\text{-Na}_2\text{HPO}_4$ buffer at pH 4.4, (B) ACN/30
468 mM $\text{H}_3\text{PO}_4\text{-Na}_2\text{HPO}_4$ buffer at pH 5.0 = 40/60 (v/v).

469 **Fig. 7.** Separation of egg white on the $\text{VC}_{18}\text{HIm}^+\text{Br}^-$ hybrid monolithic capillary
470 column by CEC. Experimental conditions: column dimension, $20\text{ cm} \times 100\text{ }\mu\text{m}$ i.d.;
471 injection, -10.0 psi for 15 s; separation voltage, -3 kV; detection wavelength, 210 nm;
472 mobile phase, 40 mM $\text{H}_3\text{PO}_4\text{-Na}_2\text{HPO}_4$ buffer at pH 4.0.

473

474

Table 1. Effects of Synthesis Parameters on the Formation of the VC₁₈HIm⁺Br⁻ Monoliths

| Column | VTES μL | Water μL | CTAB mg | Temp °C | Surface morphology | Permeability (×10 ⁻¹⁴ m ²) |
|--------------------|------------|-------------|------------|------------|---------------------------------|------------------------------------------------------|
| A1 (B1, C1, D1) | 200 | 110 | 5 | 40 | homogeneous non-transparent | 5.28 |
| A2 | 150 | 110 | 5 | 40 | homogeneous semi-transparent | 3.82 |
| A3 | 250 | 110 | 5 | 40 | Stratified | blocked |
| B2 | 200 | 50 | 5 | 40 | detached | /* |
| B3 | 200 | 140 | 5 | 40 | /** | /** |
| C2 | 200 | 110 | 3 | 40 | inhomogeneous transparent | 1.98 |
| C3 | 200 | 110 | 9 | 40 | slacked | 15.64 |
| D2 | 200 | 110 | 5 | 35 | nonrigid | /* |
| D3 | 200 | 110 | 5 | 45 | homogeneous non-transparent | blocked |

a) Other components of the prepolymerization mixture: TMOS, 300 μL; i-PrOH, 500 μL; n-BuOH, 100 μL; IL, 150 mg; AIBN, 5 mg; 1 M ammonia water, 50 μL. ACN was used as mobile phase and the flow rate was 0.5 μL/min when calculating the permeability.

b) “/*” represents the monolith was washed out and “/**” represents the failure formation of monolith.

475

476

477

Table 2. The element analysis of the monolith

| Column | Element proportion | | |
|---------------------------------------------------------------|--------------------|-------|-------|
| | N [%] | C [%] | H [%] |
| 1 (0 mg VC ₁₈ HIm ⁺ Br ⁻) | 0.08 | 17.37 | 2.84 |
| 2 (100 mg VC ₁₈ HIm ⁺ Br ⁻) | 1.18 | 21.61 | 3.38 |
| 3 (125 mg VC ₁₈ HIm ⁺ Br ⁻) | 1.39 | 25.09 | 3.97 |
| 4 (150 mg VC ₁₈ HIm ⁺ Br ⁻) | 1.66 | 27.76 | 4.37 |

478

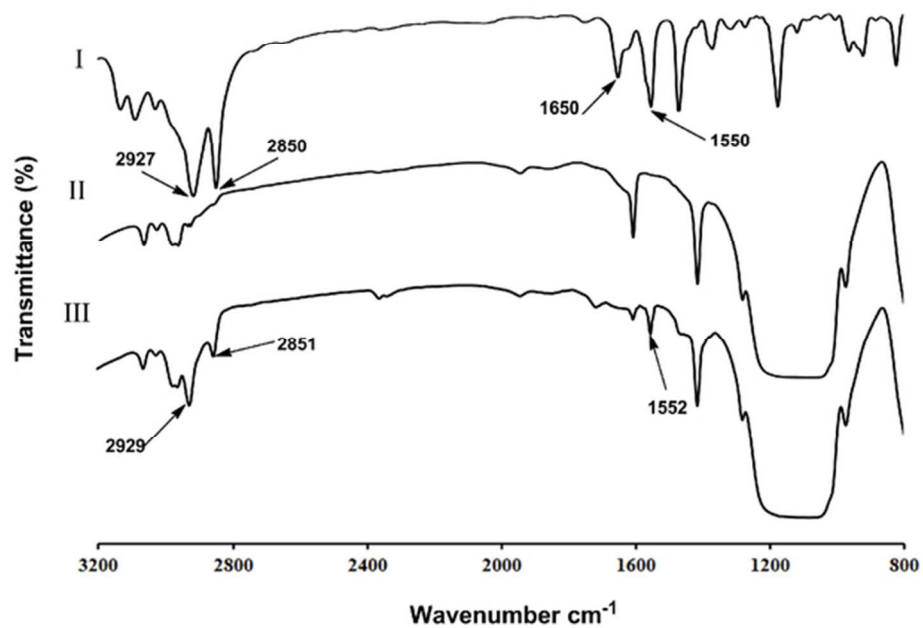


Fig. 1. FT-IR spectra of (I) IL (VC18HIm+Br-), (II) the silica-based monolith without IL and (III) the VC18HIm+Br- hybrid monolith.
56x39mm (300 x 300 DPI)

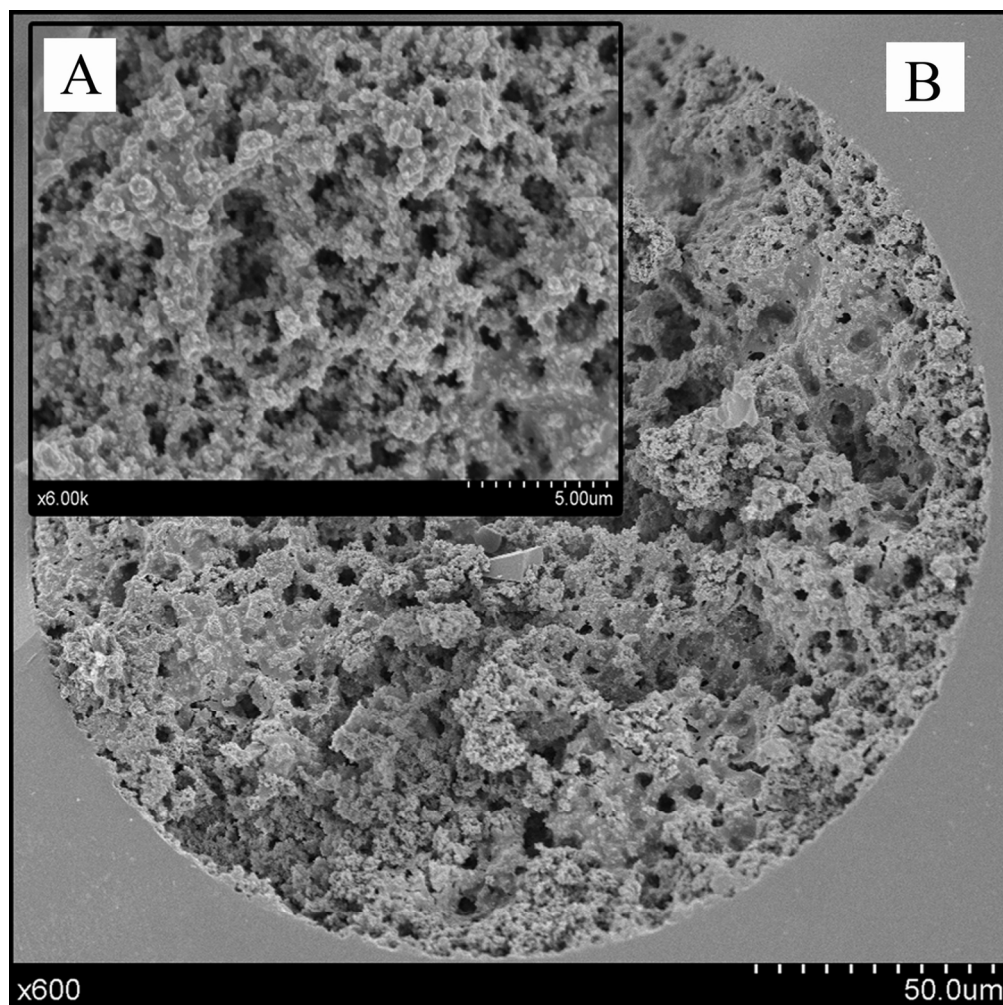


Fig. 2. SEM images of VC18HIm+Br- hybrid monolithic capillary column with optimal condition.
Magnification: (A) $\times 6000$ and (B) $\times 600$.
63x63mm (600 x 600 DPI)

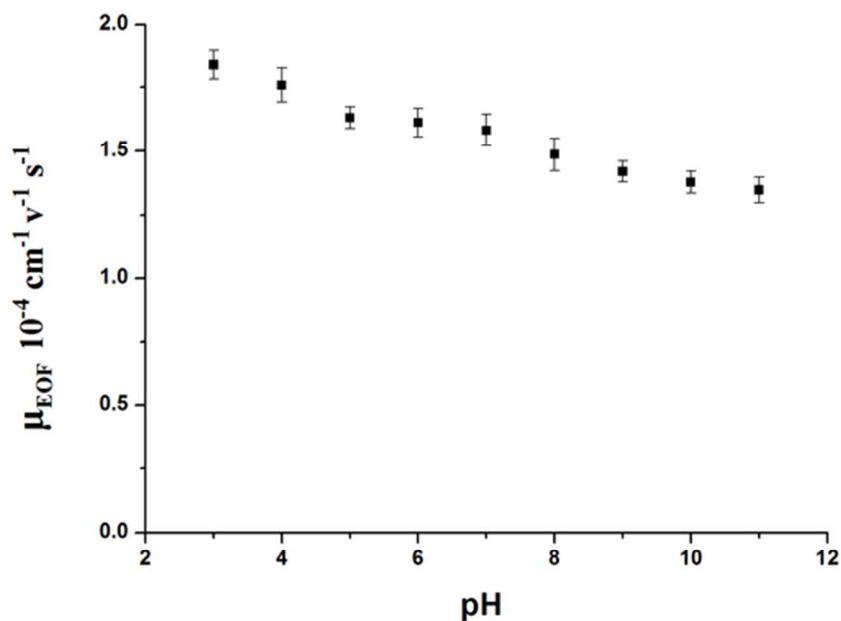


Fig. 3. Effect of pH on EOF of the VC18HIm+Br[−] hybrid monolithic capillary column. Experimental conditions: column dimension, 20 cm × 100 μm i.d.; injection, −0.5 psi for 5 s; mobile phase, 30 mM phosphate buffer (H₃PO₄–Na₂HPO₄ for pH 3.0–5.0, Na₂HPO₄–NaH₂PO₄ for pH 5.0–9.0, Na₂HPO₄–NaOH for 9.0–11.0) containing 30% ACN; void time marker of EOF, thiourea; separation voltage, −10 kV; detection wavelength, 214 nm.
56x40mm (300 × 300 DPI)

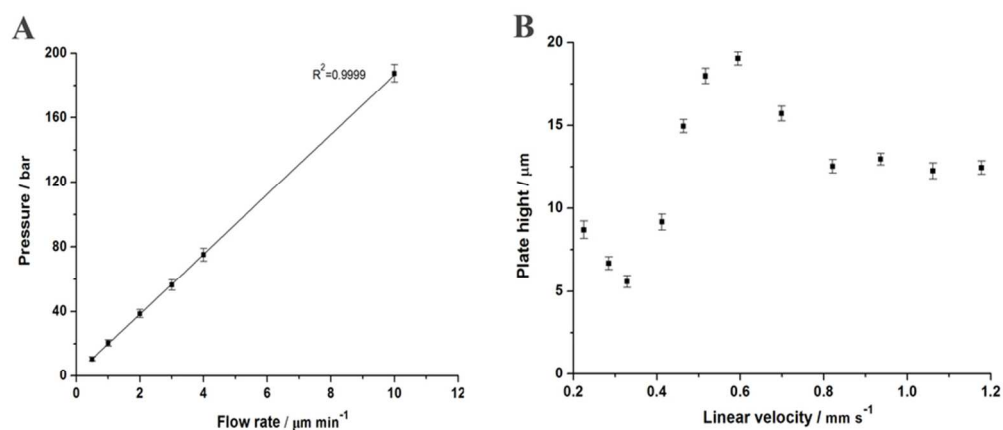


Fig. 4. (A) The mechanical stability of the VC18HIm+Br- hybrid monolithic capillary column and (B) relationship between linear velocity and the plate height of the prepared column. Experimental conditions: (A) column dimension, 20 cm \times 100 μm i.d.; flow rate 0.5 $\mu\text{L min}^{-1}$ –10 $\mu\text{L min}^{-1}$ for ACN; (B) column dimension, 20 cm \times 100 μm i.d.; injection, -0.5 psi for 5 s; mobile phase, ACN/30 mM acetic acid buffer at pH 3.0 = 30/70 (v/v); separation voltage, from -4 kV to -10 kV; detection wavelength, 214 nm. 80x37mm (300 \times 300 DPI)

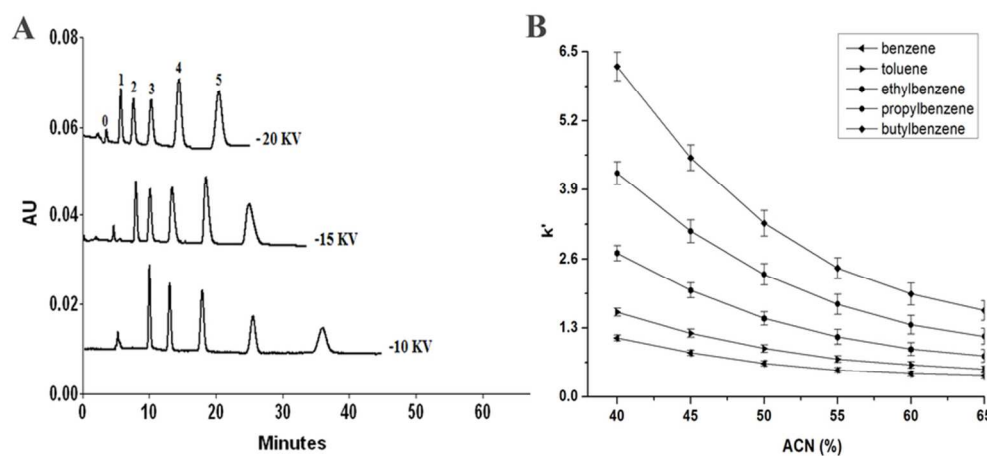


Fig. 5. (A) Separation of alkylbenzenes on the VC18HIm+Br⁻ hybrid monolithic capillary column at different separation voltage by CEC and (B) effect of ACN content in the mobile phase on the retention factors of alkylbenzenes. Solutes: (A), (0) thiourea, (1) benzene, (2) toluene, (3) ethylbenzene, (4) propylbenzene, (5) butylbenzene. Experimental conditions: column dimension, 20 cm × 100 μm i.d.; mobile phase: (A) ACN/30 mM acetic acid buffer at pH 3.0 = 40/60 (v/v), (B) different content ACN in 30 mM acetic acid buffer at pH 3.0; injection, -0.5 psi for 5 s; separation voltage: (A) different voltage, (B) -10 kV; detection wavelength, 214 nm.

80x37mm (300 × 300 DPI)

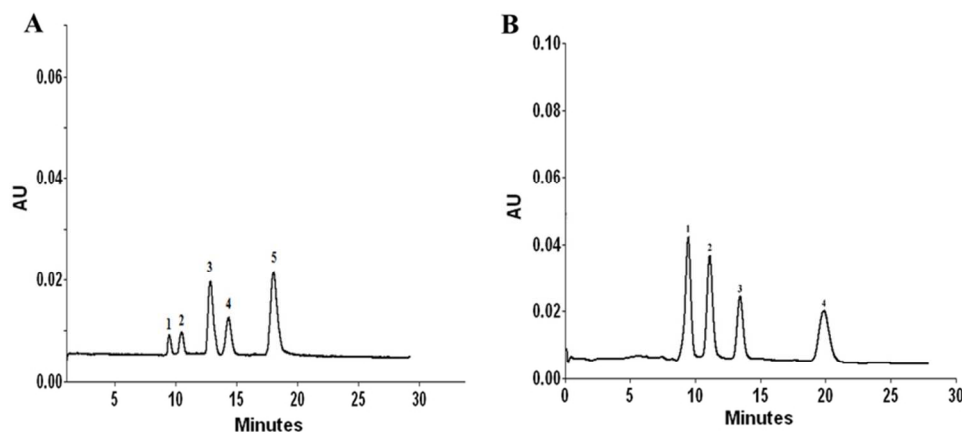


Fig. 6. (A) Separation of amino acids and (B) basic compounds on the VC18HIm+Br⁻ hybrid monolithic capillary column by CEC. Solutes: (A) (1) aspartic acid, (2) glutamic acid, (3) glutamine, (4) L-proline, (5) L-phenylalanine; (B) (1) methimazole, (2) aniline, (3) gramine, (4) 1,2-diphenyl hydrazine. Experimental conditions: column dimension, 20 cm × 100 μm i.d.; injection: (A) -1.0 psi for 15 s, (B) -0.5 psi for 5 s; separation voltage: (A) -5 kV, (B) -10 kV; detection wavelength: (A) 190 nm, (B) 214 nm; mobile phase: (A) 40 mM H₃PO₄-Na₂HPO₄ buffer at pH 4.4, (B) ACN/30 mM H₃PO₄-Na₂HPO₄ buffer at pH 5.0 = 40/60 (v/v).

77x34mm (300 × 300 DPI)

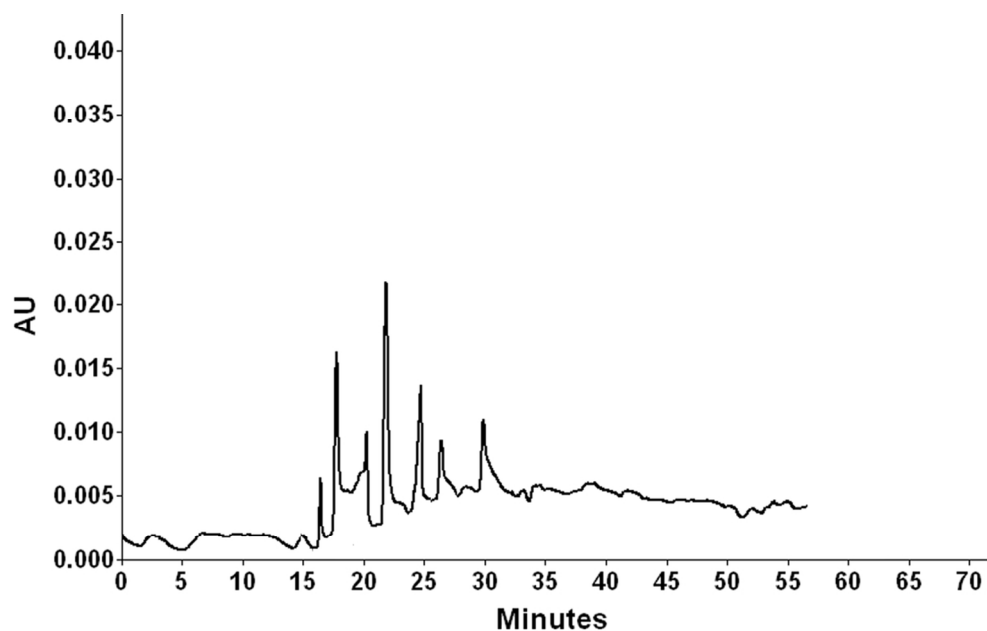
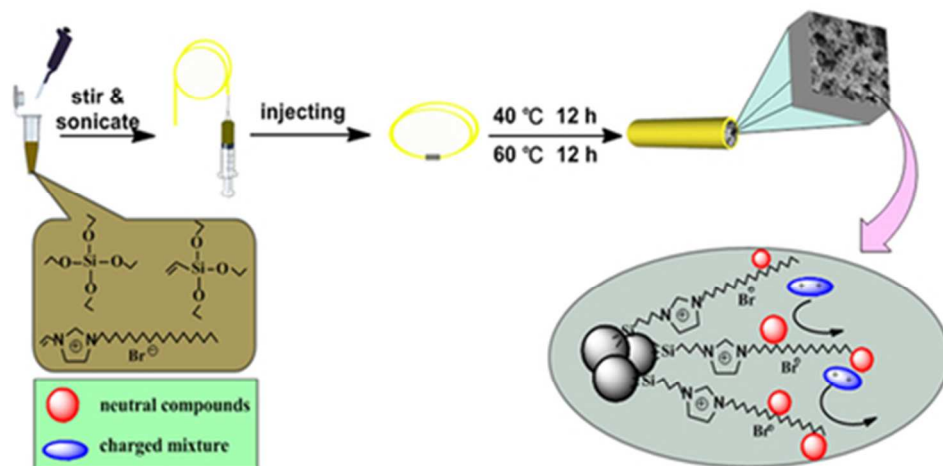


Fig. 7. Separation of egg white on the VC18HIm+Br⁻ hybrid monolithic capillary column by CEC. Experimental conditions: column dimension, 20 cm × 100 μm i.d.; injection, -10.0 psi for 15 s; separation voltage, -3 kV; detection wavelength, 210 nm; mobile phase, 40 mM H₃PO₄-Na₂HPO₄ buffer at pH 4.0. 51x32mm (600 x 600 DPI)



39x19mm (300 x 300 DPI)

Textual Abstract:

A novel IL hybrid monolithic column with great potential in separation has been fabricated via “one-pot” approach for capillary electrochromatography